OAK RIDGE NATIONAL LABORATORY
operated by
UNION CARBIDE CORPORATION
NUCLEAR DIVISION
for the
U.S. ATOMIC ENERGY COMMISSION

ORNL - TM - 2252

COPY NO. - 42

DATE - June 26, 1968

Neutron Physics Division

SENSITIVITY OF NEUTRON TRANSPORT IN OXYGEN TO VARIOUS CROSS-SECTION SETS[+]

E. A. Straker

Abstract

The effect of several input cross-section sets on the results of neutron transport in an infinite medium of oxygen is determined. The detail with which the minimum in the cross section is represented significantly affects the neutron intensity at deep penetration. The importance of using angular distributions and total cross sections determined with approximately the same energy resolution is demonstrated by results obtained by combining parts of two different cross-section sets. In addition, the effect of various amounts of smoothing of the input cross sections over energy is also shown. In general, the slope of the $4\pi R^2$ dose curves at deep penetration is determined by the minimum in the total cross section as used in the code.

NOTE:
This work supported by
DEFENSE ATOMIC SUPPORT AGENCY
under Task No. RRP-2050

[+]Submitted for journal publication.

SENSITIVITY OF NEUTRON TRANSPORT IN OXYGEN TO VARIOUS CROSS-SECTION SETS

E. A. Straker

Better techniques and instrumentation have become available in the last few years for measurements of cross sections. Thus, new structure in cross sections is being resolved as systems with better resolution are being developed. It is important to know the effect on shielding calculations of including the resolved structure in the cross sections and the importance of up-dating cross sections used in transport codes. To determine the sensitivity of transport calculations to various cross-section detail, Monte Carlo calculations have been made for the transport of fission neutrons in oxygen.

Oxygen was chosen because of the existence of a recent evaluation of its cross sections and because of the deep valleys in the total cross section. Uncollided flux measurements[1] showed that an adequate representation of the minima in the total cross sections was available in the evaluation by Slaggie and Reynolds.[2] In that evaluation, the total cross section in the deep valley at 2.37 MeV was not measured but was calculated from phase shift analysis of the angular distributions. Thus the total and differential scattering cross sections are consistent in this energy region.

A Monte Carlo code was chosen because it was absolutely necessary to use a code which utilizes the complete detail available in the cross sections, an advantage which outweighed the disadvantage of statistical variations in the result. The use of Monte Carlo, however, prevents the determination of differences of a few percent in the results at deep penetration and does not allow detailed comparisons of differential quantities without considerable machine time.

The Monte Carlo system selected was O5R-ACTIFK,[3,4] and the transport calculations were performed for an isotropic point fission source in an infinite medium of liquid oxygen. Various cross-section sets were used; a set includes the total and all the partial cross sections in a given evaluation. The three basic sets of cross sections are denoted by "KAPL," "O5R," and "UNC" and are taken from references 2, 5, and 6, respectively.

The variance reduction techniques employed were the exponential transform and modified source energy selection. A boundary crossing estimator was used with spherical boundaries between 0 and 450 cm. Flux-to-dose conversion factors of Henderson[7] were used to determine the single-collision tissue dose.

Wide variations in the results of $4\pi R^2$ dose are noted in Fig. 1. For attenuations of less than a factor of 25 there is little difference between results obtained with the KAPL and O5R cross sections; however, the results obtained with the UNC cross sections are low even for small attenuations. The shape of the $4\pi R^2$ dose curve is exponential for small attenuations and then goes through a transition region before becoming exponential again at large attenuations.

The uncollided components of the dose curves for these three sets of cross sections are shown in Fig. 2 and have the same general shape as those in Fig. 1, although the maximum contribution of the uncollided dose at deep penetration is only 10% of the total dose. Plots of the total cross sections as used in the code are shown in Fig. 3. The differences in the detailed shapes of the cross section are readily noted.

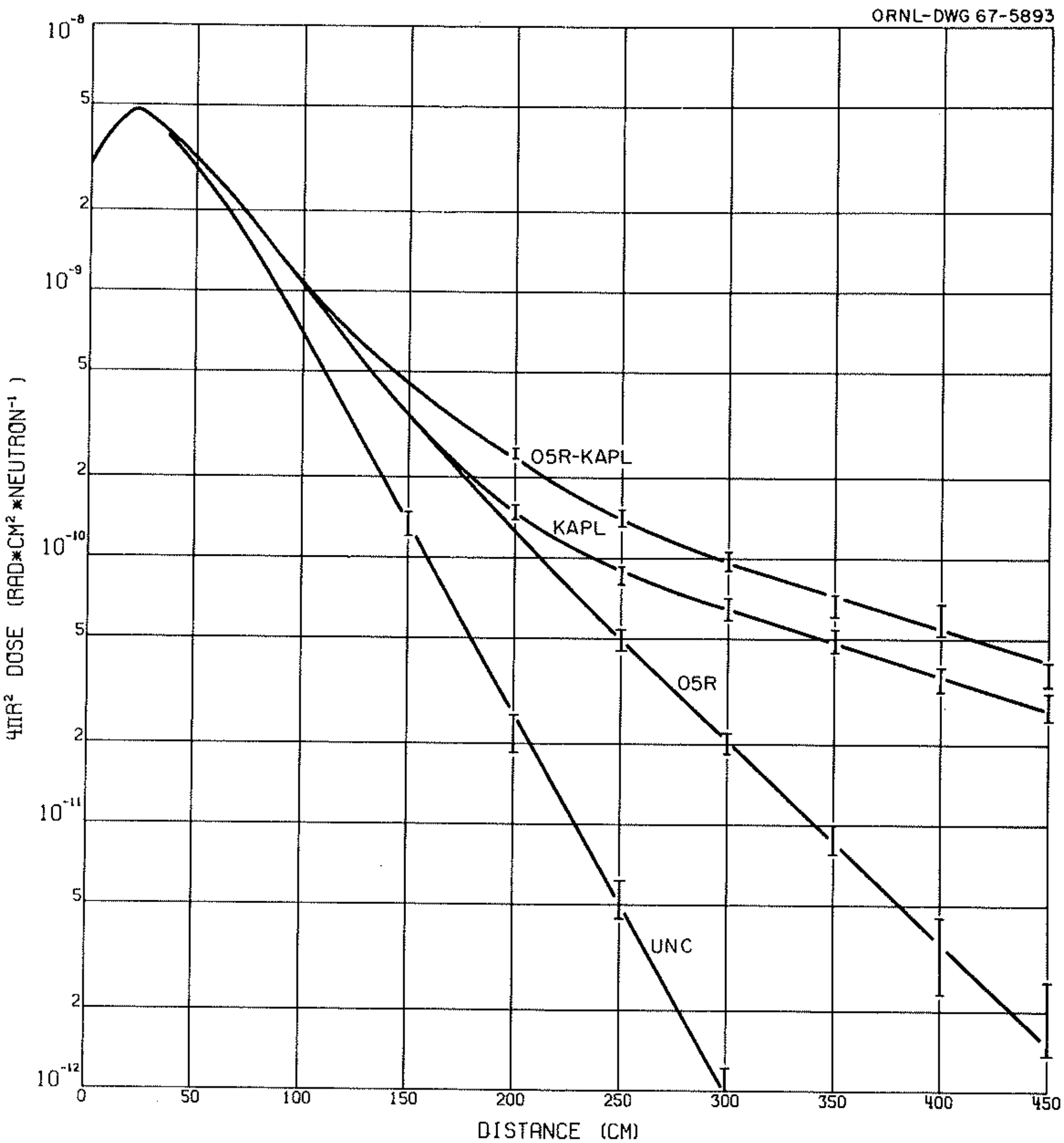

Fig. 1. $4\pi R^2$ Dose Versus Range for a Point Isotropic Fission Source in an Infinite Medium of Oxygen.

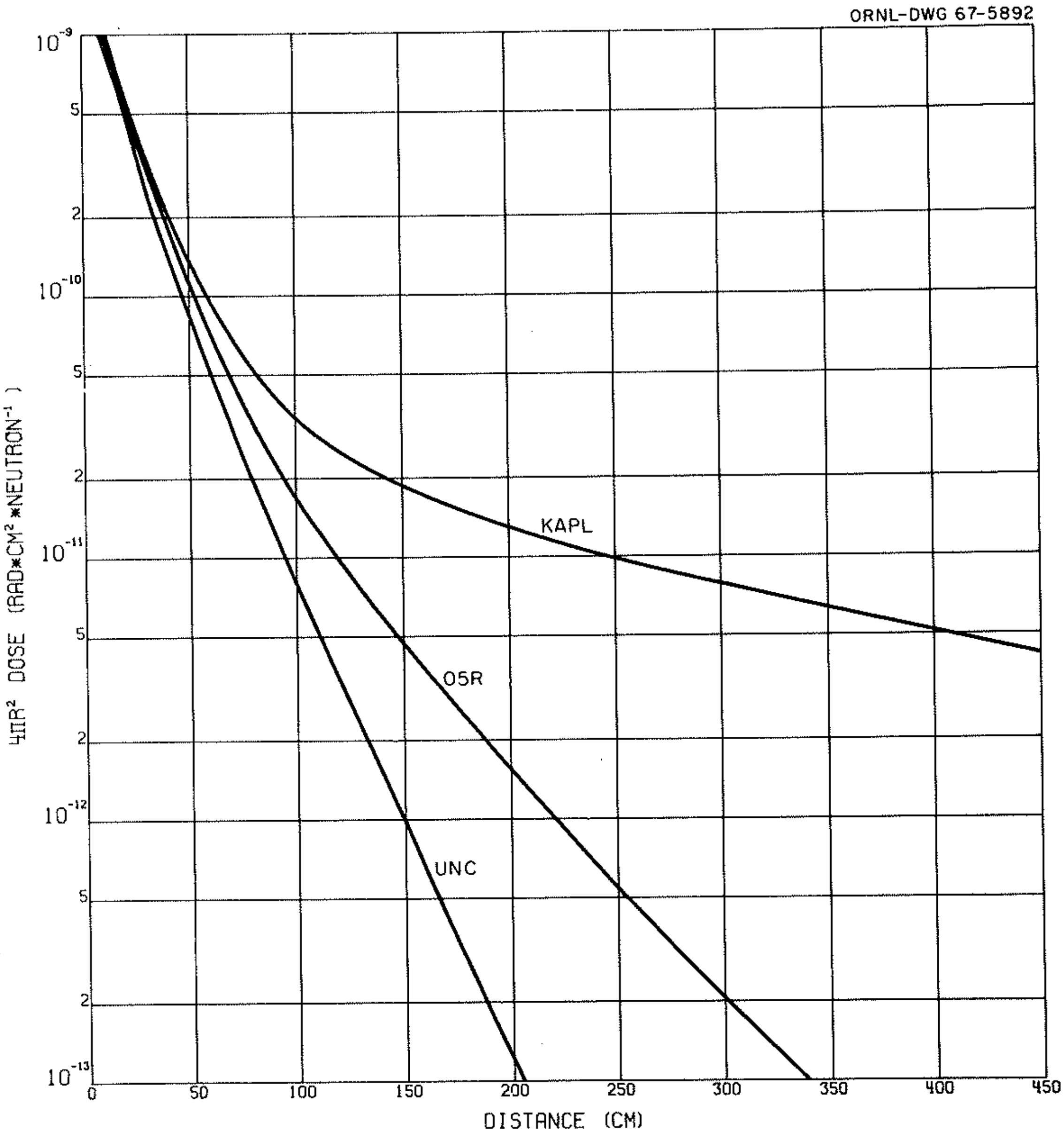

Fig. 2. $4\pi R^2$ Uncollided Dose Versus Range for a Point Isotropic Fission Source in an Infinite Medium of Oxygen.

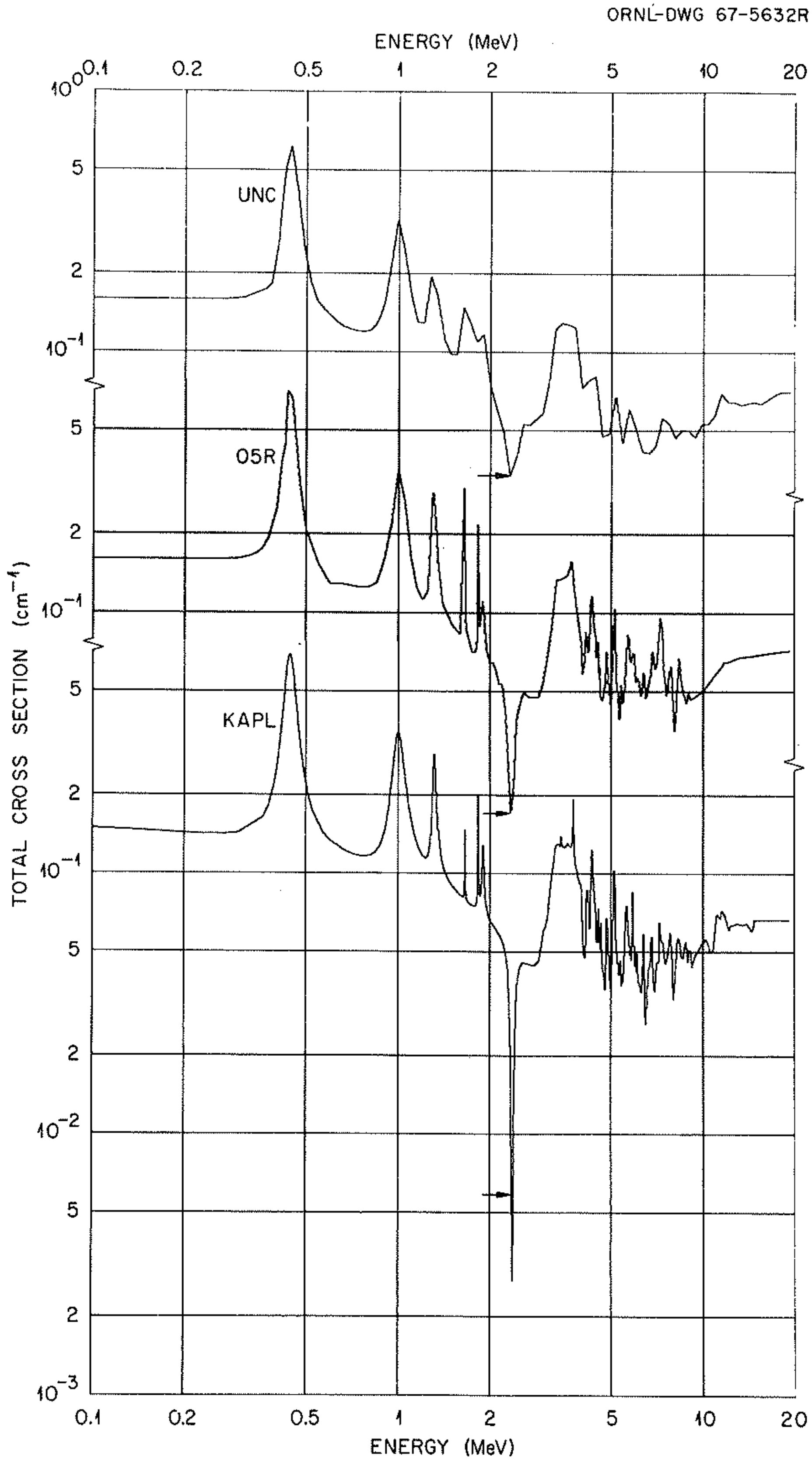

Fig. 3. O5R Representation of Various Total Cross-Section Sets for Oxygen.

To determine the importance of the partial cross sections one can arbitrarily change one portion of the cross section and determine its effect on the neutron transport. Another possibility is to substitute a partial cross section from one evaluated set into another set to determine its effect. In Fig. 1 the results obtained by substituting the 05R angular distribution data into the KAPL cross-section set are shown by the curve labeled 05R-KAPL. It is noted that the 05R-KAPL curve approaches the same slope at deep penetration as the KAPL curve but the dose is higher by a factor of approximately 1.5. Thus the total cross section still controls the shape of the curve at deep penetration but the magnitude is strongly influenced by the angular distribution of elastic scattering.

Figure 4 compares the average cosine of the scattering angle for the 05R, UNC, and KAPL cross-section information as used in the code. It is noted that in the region of the minima (2.37 MeV) the average cosine of scattering in the 05R set is approximately 0.25, whereas the average cosine in the KAPL set is nearly zero. Thus the use of the 05R angular distribution allows the neutrons to lose on the average less energy per scattering and they remain in the valley region for more scatterings; i.e., the minimum escape probability is less. Thus the angular distribution affected the magnitude of the dose but not its spatial dependence at deep penetration. It should be pointed out that the KAPL curve represents the most meaningful absolute value of the dose versus range since the total cross section was calculated from the phase shift data obtained from angular distribution measurements and was checked experimentally. However, no experimental data for dose are available for a direct comparison.

The energy spectra at a depth of 150 cm is shown in Fig. 5. The statistics are generally better than 20%. At this depth the UNC dose curve in Fig. 1 is

ORNL-DWG 67-5633R

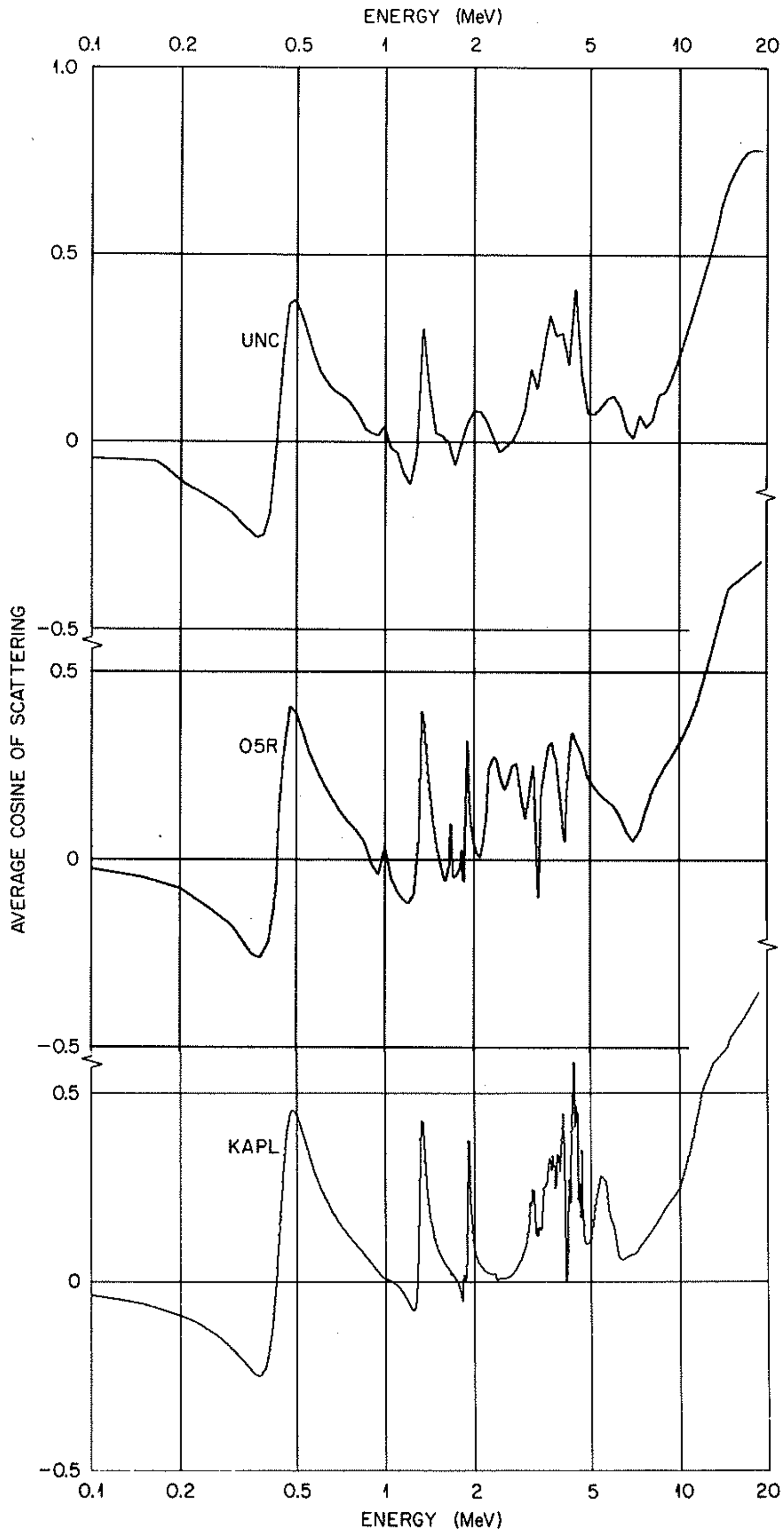

Fig. 4. O5R Representation of Various Sets of Average Cosine of the Scattering Angle for Oxygen.

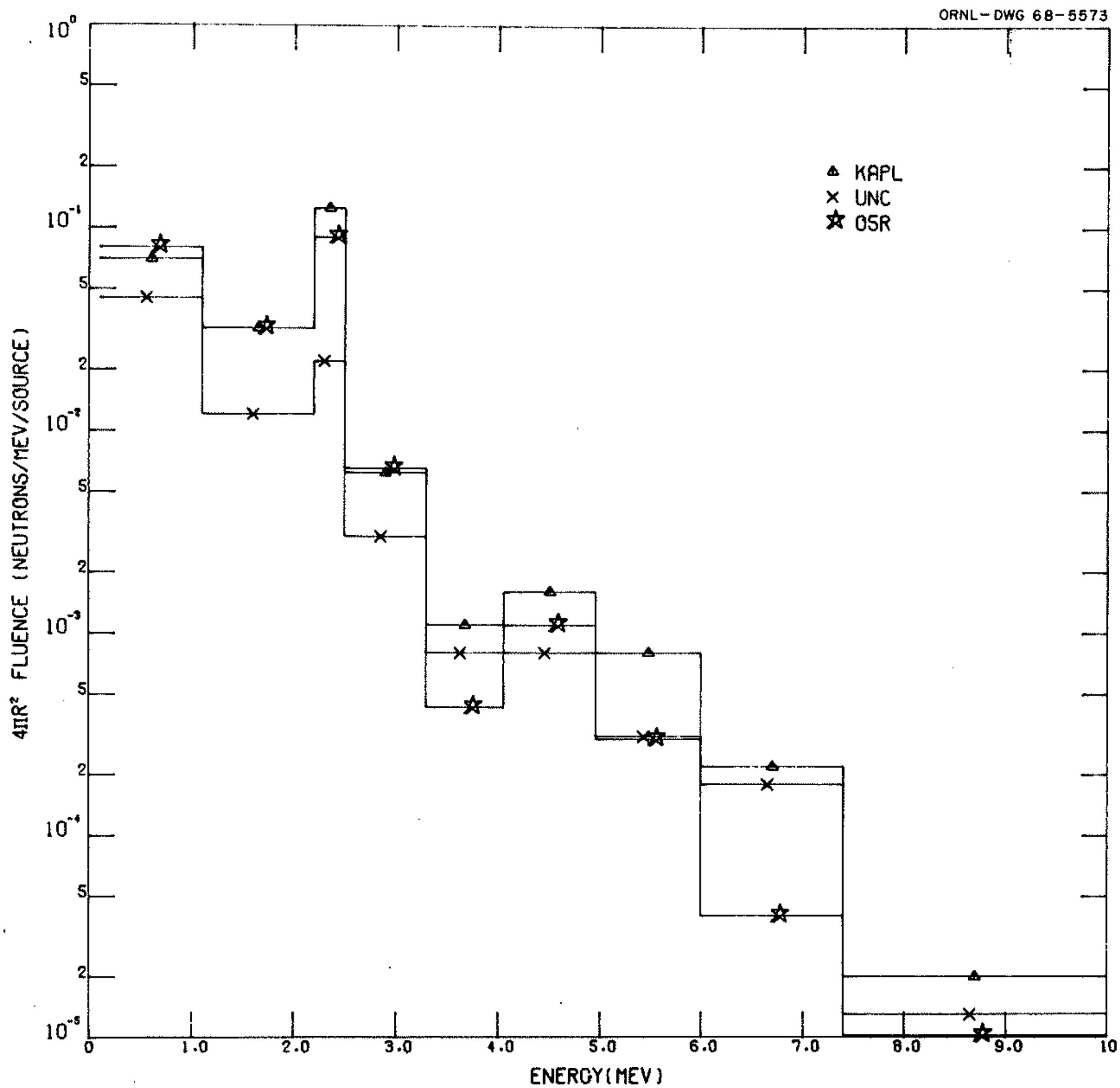

Fig. 5. $4\pi R^2$ Fluence Versus Energy at a Depth of 150 cm.

significantly lower than the O5R and KAPL curves. It is noted in Fig. 5 that there are even greater differences in the energy spectra. But even when the doses are approximately the same (O5R and KAPL) there can be large differences in the spectra. The lower KAPL cross sections in the 5- to 7-MeV range results in a higher flux in this range; the same holds for the 2.2- to 2.5-MeV range.

The determination of a detailed set of cross sections is, of course, only part of the solution of a transport problem; these cross sections must also be adequately represented in the code. To determine how much of the detail is important, calculations were performed with the KAPL cross sections after various amounts of averaging. The cross sections as used in the code are constant over an energy range which is determined by the number of points per supergroup (a supergroup is a factor of 2 in energy). Table I lists the neutron energy range and the energy interval over which the cross section is constant when various numbers of points are used. Note that for 128 points a cross section is given for every 9.41 keV in the region of the minima at 2.37 MeV. Graphs of the corresponding total cross sections as used in the code are shown in Fig. 6 and illustrate the removing of detail due to smoothing.

The results of the calculations with the various amounts of averaging are shown in Fig. 7. At 400 cm a variation in the $4\pi R^2$ dose of over a factor of 50 results from the use of 128 or 8 points per supergroup. This variation is large enough to encompass the O5R results shown in Fig. 1.

It is noted that as the cross-section detail is lost due to averaging of data points, the slope of the $4\pi R^2$ dose curve at deep penetration increases. It is believed, however, that 128 points per supergroup adequately represents the detail needed to represent the cross sections that are currently available. Thus the shape of $4\pi R^2$ dose versus distance at deep penetration is determined

Table I. Energy Interval Over Which KAPL Cross Sections Were Kept Constant

Neutron Energy (MeV)	Width of Constant Cross Section Interval (keV)		
	128 Points	32 Points	8 Points
> 9.64	75.3	301	1.205
4.82-9.64	37.5	150	600
2.41-4.82	18.8	75.3	301
1.205-2.41	9.41	37.5	150
.602-1.205	4.70	18.8	75.3
.301-.602	2.35	9.41	37.5
.150-.301	1.17	4.70	18.8
.075-.150	.585	2.35	9.41

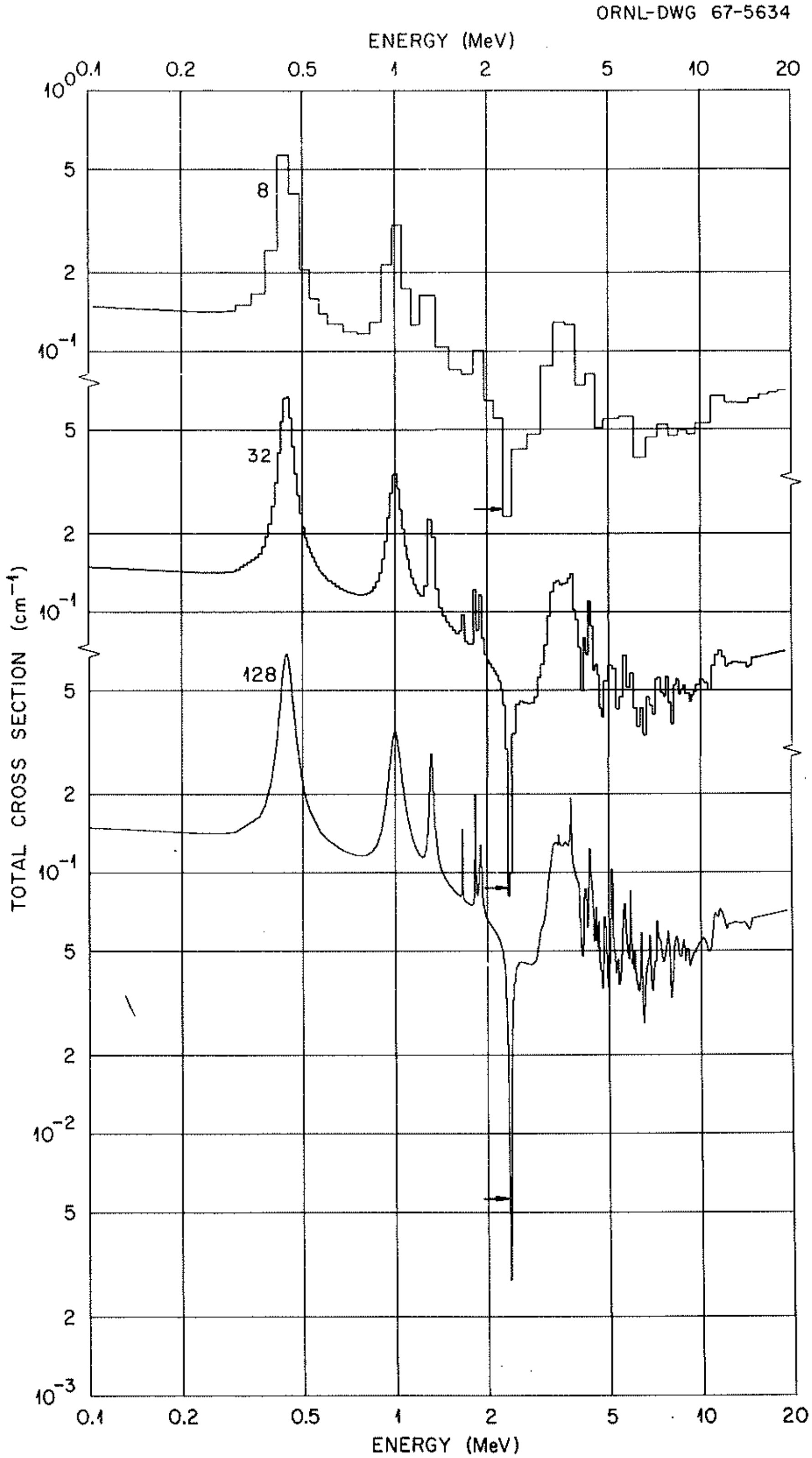

Fig. 6. O5R Representation of the KAPL Total Cross Section after Various Amounts of Averaging.

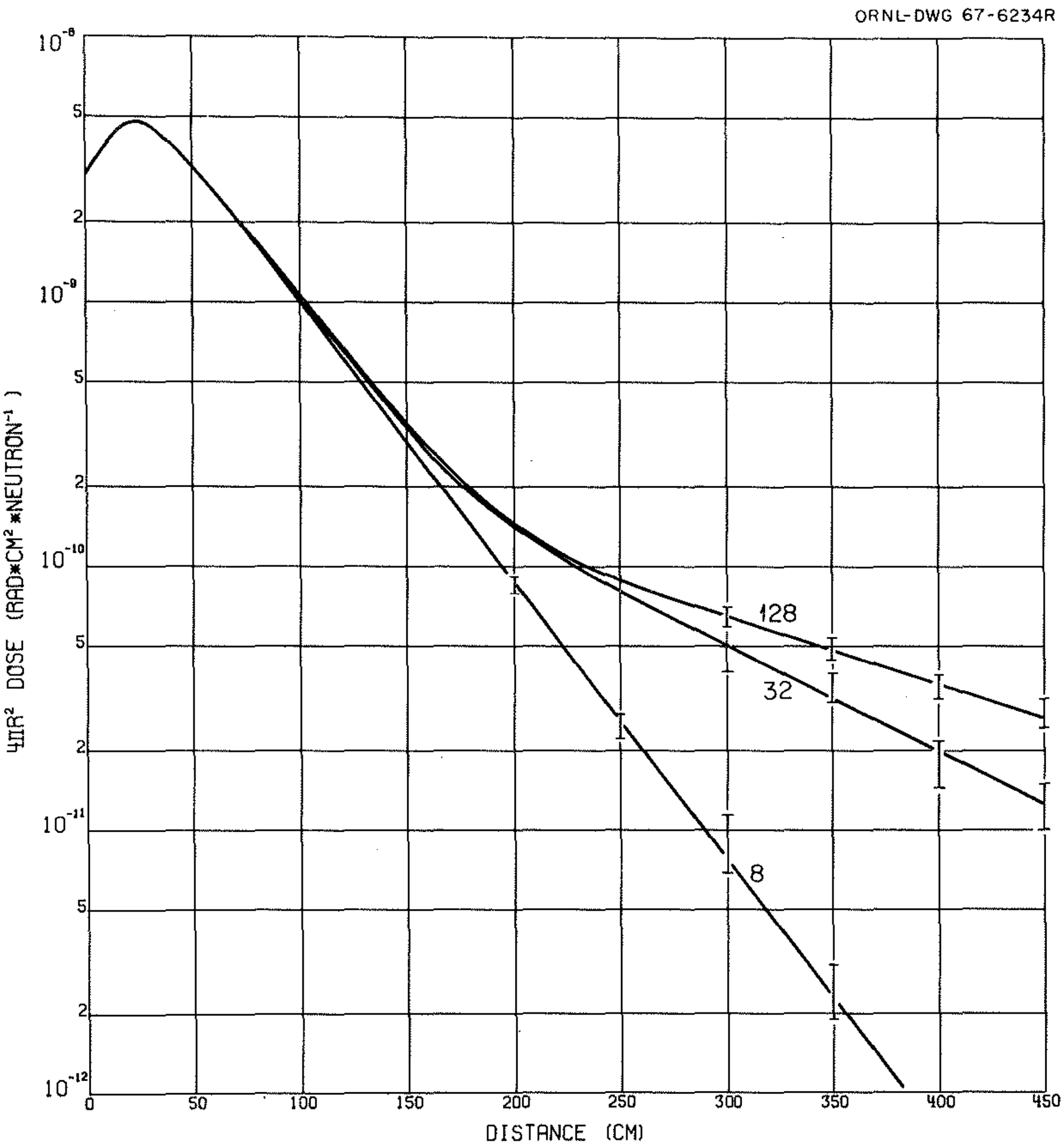

Fig. 7. The Effect of Cross-Section Averaging on $4\pi R^2$ Dose Versus Range for a Point Isotropic Fission Source in an Infinite Medium of Oxygen.

by the total cross section alone for the fission source. This is in contrast to the results of other investigations[8] which have shown that for high-energy sources the inelastic cross section controls the shape and magnitude of the dose distribution.

To illustrate that the shape of the curve is not a function of the distributed fission source alone, calculations were made for both 3- and 14-MeV monoenergetic sources (see Fig. 8). The same shape results as for a fission source. Note that the dose due to a 3-MeV source at 400 cm is approximately a factor of 3 higher than that due to a 14-MeV source. This is due to neutron removal by the charged-particle reactions in oxygen for the higher energy sources.

The slope of $4\pi R^2$ dose versus distance at deep penetrations appears to approach an exponential. This slope has been determined in terms of a macroscopic cross section and has been represented as an arrow in Figs. 3 and 6. The fact that the slope agrees quite well with the minima in the macroscopic cross-section set for each representation of the cross section clearly indicates that the minima control the transport. Only for the detailed (128-point) cross-section data of KAPL is the arrow significantly higher than the minima.

The sensitivity of the determination of neutron dose in an infinite medium of oxygen to the input cross-section set clearly illustrates the need of adequately representing the cross sections in codes for performing shielding calculations at deep penetration. The magnitude of the dose is very sensitive to the partial cross sections; the shape of the curve versus distance is determined by the detail of representation of the minima in the total cross section. The importance of having a consistent representation of the total and elastic scattering angular distribution of the cross section has been illustrated by combining parts of various cross-section sets.

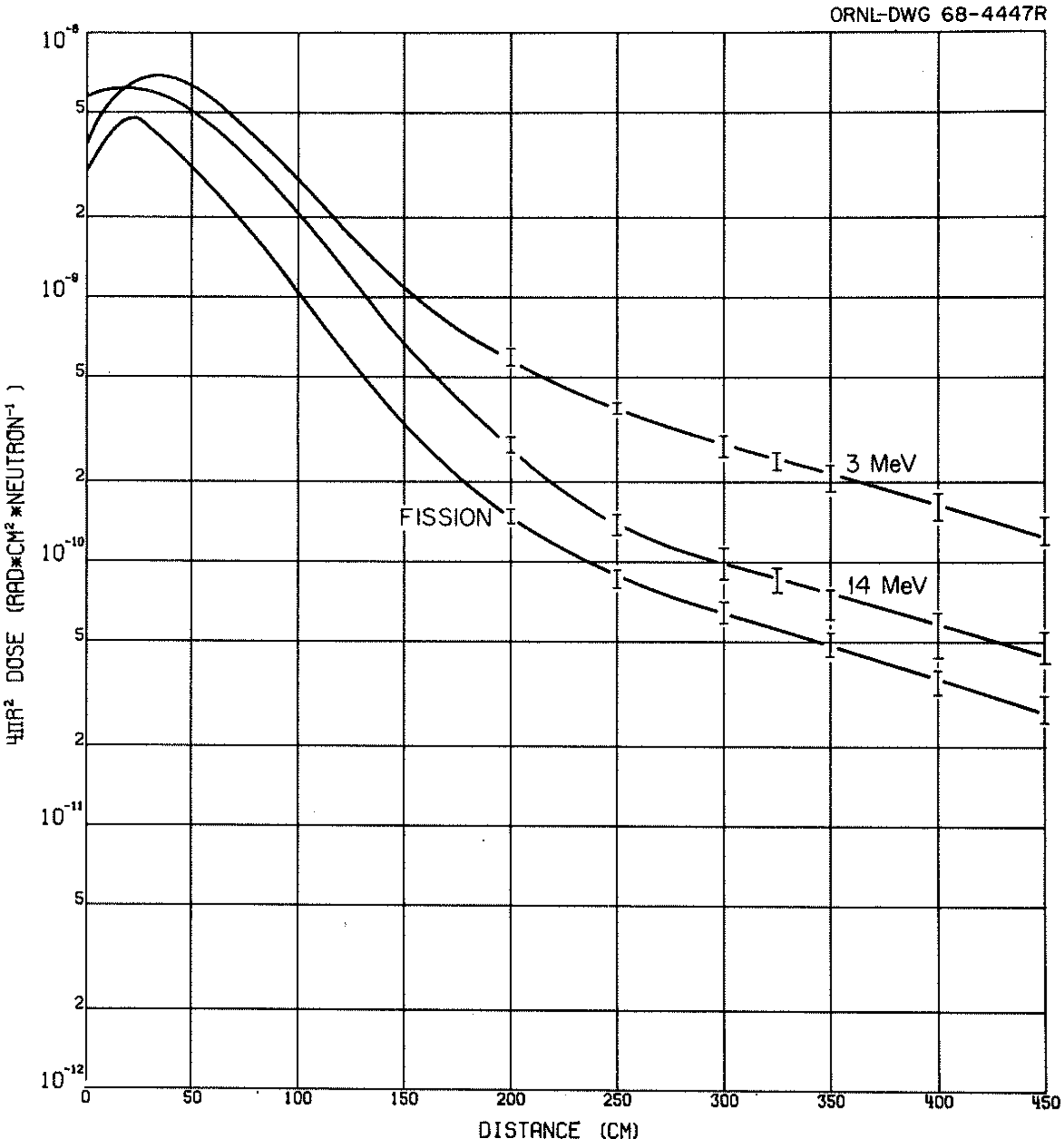

Fig. 8. $4\pi R^2$ Dose Versus Range for Point Isotropic 3- and 14-MeV Monoenergetic Sources and a Point Isotropic Fission Source in an Infinite Medium of Oxygen.

References

1. C. E. Clifford et al., "Measurements of the Spectra of Uncollided Fission Neutrons Transmitted Through Thick Samples of Nitrogen, Oxygen, Carbon, and Lead: Investigation of the Minima in Total Cross Sections," Nucl. Sci. Eng. 27, 299 (1967).

2. E. L. Slaggie and J. T. Reynolds, O-16 Fast Neutron Cross Section and Legendre Moments, KAPL-M-6452, Knolls Atomic Power Laboratory (1965).

3. D. C. Irving et al., 05R, A General-Purpose Monte Carlo Neutron Transport Code, ORNL-3622, Oak Ridge National Laboratory (1965).

4. F. B. K. Kam and K. D. Franz, ACTIFK, A General-Purpose Analysis Code for 05R, ORNL-3856, Oak Ridge National Laboratory (1966).

5. D. C. Irving, 05R Cross Section Library Memo 2, Radiation Shielding Information Center, Oak Ridge National Laboratory, Code Package CCC-17 (1965).

6. J. H. Ray, G. Grochowski, and E. S. Troubetzkoy, Neutron Cross Sections of Nitrogen, Oxygen, Aluminum, Silicon, Iron, Deuterium, and Beryllium, UNC-5139, United Nuclear Corporation (1965).

7. B. J. Henderson, Conversion of Neutron or Gamma-Ray Flux to Absorbed Dose Rate, XDC 59-8-179 (1959).

8. E. A. Straker, Calculations of the Transport of Neutrons from Fission and 14-MeV Point Sources in an Infinite Medium of Air, ORNL TM-1547, Oak Ridge National Laboratory (1966).

DASA Initial Radiation Distribution

Director, Advanced Research Projects Agency, Washington, D.C. 20301, ATTN: Project Defender

Director, Defense Atomic Support Agency, ATTN: APTL (2 copies), DDST (Mr. Hass for N-4) (4 copies), STRA (4 copies), Washington, D.C. 20305

Commander, Field Command, DASA, Sandia Base, Albuquerque, New Mexico 87115

Officer in Charge, Livermore Division, Field Command, DASA, Lawrence Radiation Laboratory, Livermore, California 94551

Director, Defense Communications Agency, Washington, D.C. 20305

Director, Defense Intelligence Agency, ATTN: DIAAP-8B, Washington, D.C. 20301 (2 copies)

Office of Defense Research and Engineering, Assistant Director (Nuclear Programs), Room 3 E1071, The Pentagon, Washington, D.C. 20301

Commanding Officer, U. S. Army Combat Developments Command, Institute of Nuclear Studies, Fort Bliss, Texas 79916

Director, U. S. Army Ballistic Research Laboratories, ATTN: Mr. E. O. Baicy, Aberdeen Proving Ground, Maryland 21005

Director of Research and Development, Department of the Army, ATTN: NIKE-X & Space, Washington, D.C. 20310

Commanding General, U. S. Army Electronics Command, Fort Monmouth, New Jersey 07703, ATTN: Institute for Exploratory Research (1 copy), Weapons Effects Section (1 copy)

Commanding Officer, U. S. Army Engineer Research & Development Laboratory, ATTN: OMEFB-EP (Mr. Dinger), Fort Belvoir, Virginia 22060

Commanding Officer, Harry Diamond Laboratories, ATTN: Chief, Nuclear Vulnerability Branch, Washington, D.C. 20438

Commanding General, U. S. Army Materiel Command, ATTN: AMCRD-BN-RE/ Nuclear Branch, Washington, D.C. 20315

NIKE-X Project Office, U. S. Army Materiel Command, Redstone Arsenal, Huntsville, Alabama 35809

Commanding Officer, U. S. Army Nuclear Defense Laboratory ATTN: Mr. Rigotti, Mr. Futterer, Edgewood Arsenal, Maryland 21010 (2 copies)

Commanding General, U. S. Army NIKE-X Systems Office, 206 N. Washington Street, Alexandria, Virginia 22314

Chief of Naval Operations, Department of the Navy, ATTN: OP 75, Washington, D.C. 20350

Commander, Naval Ordnance Laboratory, White Oak, Silver Spring, Maryland 20910

Commanding Officer, Naval Radiological Defense Laboratory, ATTN: E. Alpen, E. Tochilin, R. Shnider, J. Ferguson, San Francisco, California 94135 (4 copies)

Chief of Naval Research, Department of the Navy, Washington, D.C. 20360

Director, Naval Research Laboratory, ATTN: Mr. L. Birks, Washington, D.C. 20390

Commander, Naval Ships Systems Command, Department of the Navy, ATTN: L. E. Seiffert, Washington, D.C. 20360

Commanding Officer, Naval Weapons Evaluation Facility, Kirtland AFB, Albuquerque, New Mexico 87117

Director, Special Projects Office, Department of the Navy, Washington, D.C. 20360

AFWL, Kirtland AFB, ATTN: Major Cupka, Capt Spitale, Capt Kennedy, Dr. Darrah, Capt Hale, Capt Erkla, Major Whitaker, New Mexico 87117 (7 copies)

Commander, Air Defense Command, Ent Air Force Base, ATTN: Director of Space Defense (90SD), Colorado Springs, Colorado 80912

Commandant, AF Institute of Technology, Wright-Patterson AFB, Ohio 45433

Space & Missiles Systems Organization (SAMSO), Los Angeles Air Force Station, AF Unit Post Office, ATTN: SMTN, SMTSM-1, SNQNS-1, Los Angeles, California 90045 (3 copies)

Headquarters, U. S. Air Force, ATTN: AFGOAS, AFRDQPO, Washington, D.C. 20330 (2 copies)

University of California, Lawrence Radiation Laboratory, P. O. Box 808, ATTN: Walt Webster, L. F. Wouters, Lawrence Germain, R. Howerton, Livermore, California 94551 (4 copies)

University of California, Los Alamos Scientific Laboratory, P. O. Box 1663, ATTN: Wendell Biggers, J. S. Malik, Henry Sandmeier, Herman Hoerlin, Los Alamos, New Mexico 87544 (4 copies)

President, Sandia Corporation, P. O. Box 5800, ATTN: Clarence Mehl, Jack Walker, Albuquerque, New Mexico 87115 (2 copies)

Sandia Corporation, Livermore Laboratory, P. O. Box 969, Livermore, California 94550

Director, Division of Military Application, U. S. Atomic Energy Commission, Washington, D.C. 20545

Aerospace Corporation, San Bernadino Operation, ATTN: Dr. Chuck Greenhow, Dr. Fred Finlayson, Dr. Vic Blankenship, San Bernadino, California 92402 (3 copies)

Battelle Memorial Institute, 505 King Avenue, ATTN: Radiation Effects Information Center, Columbus, Ohio 43201 (2 copies)

Bell Telephone Laboratories, Inc., Whippany Road, ATTN: Technical Report Center, Room 2A-165B/Mr. E. Oberer, NIKE-X Systems Analyses, Whippany, New Jersey 07981

EG&G, Inc., Santa Barbara Division, P. O. Box 98, Goleta, California 93017

Gulf General Atomic, P. O. Box 608, ATTN: Dr. M. Nowak, Dr. R. Schaefer, San Diego, California 92212 (2 copies)

General Dynamics/Convair, 5001 Kearny Villa Road, P. O. Box 1128, ATTN: Dr. D. Hamlin, San Diego, California 92112

General Electric Company, Missile & Space Division, Valley Forge Space Technology Center, P. O. Box 8555, Philadelphia, Pennsylvania 19101

General Electric Company, TEMPO, Center for Advanced Studies, 816 State Street, ATTN: DASA Information and Analysis Center, Santa Barbara, California 93102 (4 copies)

IIT Research Institute, 10 West 35th Street, ATTN: Dr. Adelman, Chicago, Illinois 60616

Institute for Defense Analyses, 400 Army-Navy Drive, ATTN: Technical Information Office, Arlington, Virginia 22200

Kaman Aircraft Corporation, Nuclear Division, Garden of the Gods Road, ATTN: Dr. F. Shelton, Colorado Springs, Colorado 80907

Lockheed Missiles & Space Company, 3251 Hanover Street, ATTN: R. Meyerott, Palo Alto, California 94304

Dr. Malvin H. Kalos, Courant Institute of Mathematical Sciences, 251 Mercer Street, New York, New York 10012

Mathematical Applications Group, Inc., 180 South Broadway, White Plains, New York 10605

Radiation Research Associates, 1506 West Terrell Avenue, Fort Worth, Texas 76104

The RAND Corporation, 1700 Main Street, ATTN: Dr. H. Brode, Dr. J. Marcum, Dr. W. Karzas, Santa Monica, California 90406 (3 copies)

TRW Systems, Vulnerability & Hardness Laboratory, One Space Park, Redondo Beach, California 90278 (3 copies)

United Nuclear Corporation, Grasslands Road, (Route 100C), ATTN: Dr. Schamberger, Mr. Ross, Elmsford, New York 10523 (2 copies)

INTERNAL DISTRIBUTION

1-3. L. S. Abbott
4. R. Booth
5. V. R. Cain
6. H. C. Claiborne
7. C. E. Clifford
8. R. R. Coveyou
9. R. M. Freestone
10. L. B. Holland
11. D. Irving
12. R. E. Maerker
13-14. F. C. Maienschein
15. F. J. Muckenthaler
16. R. W. Peelle
17. S. K. Penny
18. F. G. Perey
19. G. de Saussure
20. F. Schmidt
21. E. Solomito
22. P. N. Stevens
23-32. E. A. Straker
33. D. Sundberg
34. D. K. Trubey
35. K. J. Yost
36. W. Zobel
37. E. R. Cohen (consultant)
38. B. C. Diven (consultant)
39. W. N. Hess (consultant)
40. M. H. Kalos (consultant)
41. L. V. Spencer (consultant)
42-43. Central Research Library
44. Document Reference Section
45-59. Laboratory Records Department
60. Laboratory Records ORNL RC
61. ORNL Patent Office

EXTERNAL DISTRIBUTION

62. Lt. Anthony R. Buhl, USA-Nuclear Defense Laboratory, Edgewood Arsenal, Maryland 21010
63. H. Goldstein, Room 242, Mudd Building, Columbia University, New York 27, New York
64. P. B. Hemmig, Division of Reactor Development and Technology, U. S. Atomic Energy Commission, Washington, D. C.
65. F. R. Mynatt, Computing Technology Center, Oak Ridge, Tennessee
66. I. F. Zartman, Division of Reactor Development and Technology, U. S. Atomic Energy Commission, Washington, D. C.
67-162. Given DASA Initial Radiation distribution listed on preceding pages.
163-177. Divison of Technical Information Extension (DTIE)
178. Laboratory and University Division (ORO)